Redox Biology 15 (2018) 22–33

Contents lists available at ScienceDirect

Redox Biology

journal homepage: www.elsevier.com/locate/redox

Research Paper

Cholinergic anti-inflammatory pathway inhibits neointimal hyperplasia by suppressing inflammation and oxidative stress

Dong-Jie Li[a,1], Hui Fu[a,1], Jie Tong[a], Yong-Hua Li[b], Le-Feng Qu[c,*], Pei Wang[d,e,**], Fu-Ming Shen[a,*]

[a] Department of Pharmacy, Shanghai Tenth People's Hospital, Tongji University School of Medicine, Shanghai, China
[b] Department of Anesthesiology, Changzheng Hospital, Second Military Medical University, Shanghai, China
[c] Department of Vascular and Endovascular Surgery, Changzheng Hospital, Second Military Medical University, Shanghai, China
[d] Department of Pharmacology, Tongji University School of Medicine, Shanghai, China
[e] Department of Pharmacology, School of Pharmacy, Second Military Medical University, Shanghai, China

ARTICLE INFO

Keywords:
Cholinergic anti-inflammatory pathway
α7 nicotinic acetylcholine receptor
Neointimal hyperplasia
Inflammation
Oxidative stress

ABSTRACT

Neointimal hyperplasia as a consequence of vascular injury is aggravated by inflammatory reaction and oxidative stress. The α7 nicotinic acetylcholine receptor (α7nAChR) is a orchestrator of cholinergic anti-inflammatory pathway (CAP), which refers to a physiological neuro-immune mechanism that restricts inflammation. Here, we investigated the potential role of CAP in neointimal hyperplasia using α7nAChR knockout (KO) mice. Male α7nAChR-KO mice and their wild-type control mice (WT) were subjected to wire injury in left common carotid artery. At 4 weeks post injury, the injured aortae were isolated for examination. The neointimal hyperplasia after wire injury was significantly aggravated in α7nAChR-KO mice compared with WT mice. The α7nAChR-KO mice had increased collagen contents and vascular smooth muscle cells (VSMCs) amount. Moreover, the inflammation was significantly enhanced in the neointima of α7nAChR-KO mice relative to WT mice, evidenced by the increased expression of tumor necrosis factor-α/interleukin-1β, and macrophage infiltration. Meanwhile, the chemokines chemokine (C-C motif) ligand 2 and chemokine (CXC motif) ligand 2 expression was also augmented in the neointima of α7nAChR-KO mice compared with WT mice. Additionally, the depletion of superoxide dismutase (SOD) and reduced glutathione (GSH), and the upregulation of 3-nitrotyrosine, malondialdehyde and myeloperoxidase were more pronounced in neointima of α7nAChR-KO mice compared with WT mice. Accordingly, the protein expression of NADPH oxidase 1 (Nox1), Nox2 and Nox4, was also higher in neointima of α7nAChR-KO mice compared with WT mice. Finally, pharmacologically activation of CAP with a selective α7nAChR agonist PNU-282987, significantly reduced neointima formation, arterial inflammation and oxidative stress after vascular injury in C57BL/6 mice. In conclusion, our results demonstrate that α7nAChR-mediated CAP is a neuro-physiological mechanism that inhibits neointima formation after vascular injury via suppressing arterial inflammation and oxidative stress. Further, these results imply that targeting α7nAChR may be a promising interventional strategy for in-stent stenosis.

1. Introduction

Neointimal hyperplasia is a complicated cellular and molecular response characterized by aggressive proliferation following mechanical vascular injury, such as angioplasty and stenting, endarterectomy, and vein bypass graft failure [1]. This disorder leads to a narrowing of the arterial lumen known as restenosis, which limit the safety and efficacy of percutaneous transluminal coronary angioplasty and necessitates the need for retreatment [2,3]. Currently, it has been widely accepted that the abnormal proliferative phenotype of vascular smooth muscle cells (VSMCs) in the intimal region plays a key role in the development of neointimal hyperplasia after vascular injury. VSMCs always exhibit a contractile phenotype with little proliferation/migration and extracellular matrix (ECM) production under normal condition, but turn to a

Abbreviations: 3-NT, 3-nitrotyrosine; α7nAChR, α7 nicotinic acetylcholine receptor; α-SMA, α-smooth muscle actin; CAP, cholinergic anti-inflammatory pathway; CCL2, chemokines chemokine (C-C motif) ligand 2; CNS, central nervous system; CXCL2, chemokine (CXC motif) ligand 2; GSH, reduced glutathione; IL-1β, interleukin-1β; KO, knockout; MDA, malondialdehyde; MPO, myeloperoxidase; SOD, superoxide dismutase; TNF-α, tumor necrosis factor-α; WT, wild type; VSMCs, vascular smooth muscle cells

* Corresponding authors.
** Corresponding author at: Department of Pharmacology, Tongji University School of Medicine, Shanghai, China.
E-mail addresses: qulf08@126.com (L.-F. Qu), wangp249@foxmail.com (P. Wang), fumingshen@tongji.edu.cn (F.-M. Shen).
[1] These authors contribute equally to this work.

https://doi.org/10.1016/j.redox.2017.11.013
Received 25 October 2017; Received in revised form 7 November 2017; Accepted 16 November 2017
Available online 16 November 2017

synthetic phenotype after vascular injury [2,3]. Importantly, the vascular injury-induced inflammatory response, chemokines induction and oxidative stress, critically contribute to the VSMC phenotype switch and neointimal hyperplasia [4,5]. Many redox signaling factors, including nuclear factor 2 (Nrf2) [6], peroxiredoxin [7], and heme oxygenase-1 (HO-1) [8], play key roles in neointimal hyperplasia after vascular injury [4,9,10].

Nicotinic acetylcholine receptors (nAChRs) are a group of cholinergic ligand-gated ion channels that respond to the neurotransmitter acetylcholine. They also respond to many types of chemical compounds such as nicotine. The nAChRs are mainly expressed in the central nervous system (CNS) and regulate diverse biological function of CNS [11]. The α7 nicotinic ACh receptor (α7nAChR), which is also known as cholinergic receptor nicotinic α7 subunit (*CHRNA7*), is one of the most common receptors expressed in the CNS [12,13]. The α7nAChR is characterized by its rapid desensitization and high calcium permeability in cholinergic neurotransmission [12,13]. A large number of studies have pointed out that α7nAChR is not only involved in cognitive functions such as memory and learning, but also implicated in neurological disorders such as Alzheimer's diseases, Parkinson's disease, depression, and schizophrenia [12].

Interestingly, recent investigations discovered that α7nAChR is widely expressed in peripheral non-nerve cells such as lymphocytes, monocytes and macrophages, and plays an indispensable role in the "cholinergic anti-inflammatory pathway (CAP)", which refers to a physiological neuro-immune mechanism that limits innate immune function in a ACh-dependent manner [14–16]. CAP has a major contribution in alleviating both acute and chronic inflammatory pathologies such as endotoxemia and inflammatory bowel disease [14–16]. We previously reported that α7nAChR-medaited CAP is a potent protective mechanism in many disease states of cardiovascular system, including endothelial dysfunction [17], hypertension [18,19], shock [20] and vascular aging [21]. However, whether CAP participates in the development of neointimal hyperplasia after vascular injury has not been studied yet.

In the present study, we examined the function of CAP in vascular injury using α7nAChR knockout mice model, and explored the potential effects of α7nAChR deletion on inflammation and oxidative stress in the injured vascular wall.

2. Methods

2.1. Animal

The α7nAChR KO mice (*Chrna7*^{tm1Bay}, number 003232) and wild type control mice (C57BL/6) were purchased from Jackson laboratory and described in our previous studies [18,21]. The α7nAChR KO mouse strain used in this study was backcrossed to C57Bl/6 for at least six generations. The mice were bred and housed in temperature-controlled cages under a 12/12-h light/dark cycle with free access to water and chow in Tongji University Animal Core. Animals were used in accordance with the Tongji University institutional guidelines for animal care and the Guide for Care and Use of Laboratory Animals published by the US National Institutes of Health.

2.2. Arterial injury model

Transluminal arterial injury model was induced as described previously [22]. For all surgical procedures, the mice were anesthetized by intraperitoneal injection with pentobarbital sodium (50 mg/kg). Surgery was carried out using a dissecting microscope (SMZ-800, Nikon, Tokyo, Japan). A guide wire (0.38 mm in diameter) was inserted into the left common carotid artery of 8-week-old male WT or α7nAChR-KO mice. The wire was left in place for 1 min to denude and dilate the artery. Carprofen (5 mg/kg) was used for analgesia, administered subcutaneously daily for 3 days following surgery.

2.3. Drug administration

The C57BL/6 mice were divided into three groups: uninjured group, injured group and injured + PNU-282987 group. The mice in injured group underwent wire-injury as described above, while the mice in uninjured group underwent sham-operation without wire insertion. The mice in injured + PNU-282987 group underwent wire-injury and were administrated with PNU-282987 for 4 weeks. For PNU-282987 treatment, the PNU-282987 (Sigma-Aldrich, #P6499) was dissolved in 0.4% DMSO in saline was injected intraperitoneally once a day at 9 a.m. ~ 11 a.m. (1 mg/kg/d). This does was chosen according to our previous study [18,21]. The mice in injured group and uninjured groups also received injection with vehicle (0.4% DMSO in saline) at the same time.

2.4. Blood pressure measurement, tissue sampling and serum basal parameters

At 4 weeks post injury, the mice were subjected to measurement of blood pressure according to our previous report [18]. Then, mice were fasted overnight and weighted. The mice were then euthanized by intraperitoneal administration of an overdose of pentobarbital sodium (150 mg/kg, i.p.). The blood was obtained for isolating serum to determine fasting glucose and cholesterol using an automatic biochemistry analyzer (Hitachi 7020). For histological and immunohistochemistry analysis, the mice at death were perfused with 0.9% NaCl solution for 5 min followed by perfusion fixation with 4% paraformaldehyde in PBS (pH 7.4) for 15 min. The left (injured) and right (uninjured) common carotid arteries were carefully excised and further fixed in 4% paraformaldehyde overnight at 4 °C, and embedded in paraffin. For biomedical analysis, another set of mice with transluminal arterial injury were injected with pentobarbital sodium (150 mg/kg, i.p.) and perfused with 0.9% NaCl solution for 1 min to flush the blood. Then, their carotid arteries were excised swiftly and stored at −80 °C.

2.5. Histological examination

Hematoxylin and eosin (H&E) staining was used to assess morphological changes. Paraffin-embedded tissues were cut to sections (8 μm) and then paraffin was removed with xylen and tissues were washed with ethanol [23]. Then, the sections were stained in hematoxylin and eosin according to standard procedures. Collagen distribution in the aortic wall was evaluated by Masson staining [24]. Briefly, sections (8 μm) were dewaxed and rehydrated, followed by counterstaining with Weigert's iron hematoxylin (5–10 min), followed by Masson's trichrome staining solution. Sections were washed in 1% acetic acid (1 min) and dehydrated with alcohol and xylene using standard procedures.

2.6. Immunohistochemistry

Immunohistochemistry was performed as described previously [25–27]. For immunohistochemistry experiments, frozen 8-μm-thick sections were fixed in 4% paraformaldehyde. The sections were blocked by 8% normal goat serum for 4 h and then incubated in specific primary antibodies. After being washed three times by PBS, the sections were incubated with horseradish peroxidase-conjugated secondary antibodies. Staining is visualized using substrate diaminobenzidine. The following antibodies were used: α-smooth muscle actin (α−SMA, #ab7817, Abcam, Cambridge, UK, 1: 600 dilution), PCNA (clone PC10, Millipore, Milford, MA, USA, 1;1000 dilution), tumor necrosis factor-α (TNF-α, #ab9635, Abcam, Cambridge, UK, 1: 1000 dilution), interleukin-1β (IL-1β, #MAB4012, R&D Systems, Minneapolis, MN, USA, 1: 1000 dilution), CD68 (#MA5-13324, Invitrogen, Carlsbad, CA, USA, 1: 2000 dilution), 3-nitrotyrosine (3-NT, #sc-32757, 1: 4000 dilution) malondialdehyde (MDA, #ab6463, 1: 2000 dilution), myeloperoxidase (MPO, #PA5-16672, Invitrogen, 1: 2500 dilution), chemokine (C-C

motif) ligand 2 (CCL2, #MA5-17040, Invitrogen, 1: 1500 dilution) and chemokine (CXC motif) ligand 2 (CXCL2, #PA5-28820, Invitrogen, 1: 2000 dilution).

2.7. Real-time quantitative PCR

Real-time PCR for determining mRNA level was performed as described previously [18,21,28]. Total RNA was extracted from arteries using TRIzol reagent (Invitrogen, Carlsbad, CA) according to the instructions of the manufacturer. RNase-free DNase I was used to reduce the risk for genomic DNA contamination. About 2 μg RNA was reverse transcribed to cDNA using the M-MLV enzyme (Promega, Madison, WI). Real-time quantitative PCR was performed using the ABI7500 real-time PCR detection system (ABI System) and SYBR® Green Real-Time PCR Master Mixes (ABI System) with specific primers for TNF-α, IL-6, IL-1β, CCL2 and CXCL2.□□The primers were as follows: TNF-α, F: GGAAC ACGTCGTGGGATAATG, R: GGCAGACTTTGGATGCTTCTT; IL-1β, F: GAAATGCCACCTTTTGACAGTG, R: TGGATGCTCTCATCAGGACAG; CCL2, F: GTGCTGACCCCAAGAAGGA, R: GGTGGTTGTGGAAAAGGTA GTG; CXCL2, F: ACCAACCACCAGGCTACAGG, R: GCTTCAGGGTCAA GGCAAAC; CD68, F: TGTCTGATCTTGCTAGGACCG, R: GAGAGTAAC GGCCTTTTTGTGA; GAPDH, F: GTATGACTCCACTCACGGCAAA, R: GGTCTCGCTCCTGGAAGATG. The PCR reactions were initiated with denaturation at 95 °C for 10 s, followed by amplification with 40 cycles at 95 °C for 10 s, and annealing at 60 °C for 20 s (two-step method). Finally, melting curve analysis was performed from 60 °C to 85 °C. The rat glyceraldehyde 3-phosphate dehydrogenase (GAPDH) gene was used as an endogenous control. The relative expression of the target genes was normalized to the level of GAPDH in the same cDNA. All samples were performed in duplicate. The $2^{-\Delta\Delta Ct}$ method was used to comparison of mRNA levels.

2.8. Immunoblotting

Immunoblotting was performed as described previously [29–31]. Protein was extracted from tissues or cells with RIPA buffer (Beyotime, Haimen, China) supplemented with a protease/phosphatase inhibitor cocktail (Pierce Technology, Rockford, IL). After centrifugation at 12,000 g for 10 min, the supernatant was collected and boiled for 5 min in SDS-PAGE sample buffer and run on 10% SDS-PAGE. The proteins were electrotransferred to nitrocellulose membranes, probed with primary antibody overnight, and then incubated with Infrared-Dyes-conjugated secondary antibodies (Li-Cor, Lincoln, NE). The images were obtained with Odyssey Infrared Fluorescence Imaging System (Li-Cor). All immunoblotting experiments were repeated at least three times. The following antibodies were used: α-smooth muscle actin (α−SMA, Abcam, 1: 2000 dilution), PCNA (Millipore, 1:3000 dilution), 3-nitrotyrosine (3-NT, #sc-39B6, 1: 4000 dilution), NADPH oxidase 1 (Nox1, Abcam, 1:3000 dilution), Nox2 (Abcam, 1:3000 dilution), Nox4 (Abcam, 1:3000 dilution) and GAPDH (Santa Cruz Biotechnology, 1:5000 dilution).

2.9. Measurement of superoxide dismutase (SOD) and reduced glutathione (GSH) levels

After being sacrificed by overdose of pentobarbital sodium (150 mg/kg, i.p.), the injured arteries were isolated from WT and α7nAChR KO mice. The aortic tissues were homogenized swiftly and dissolved in extraction buffer for the analysis of SOD and GSH content. To measure the antioxidative enzyme activities in the injured aortic tissues, SOD and GSH levels were detected using commercial kits (Cayman Chemical, Ann Arbor, MI) following the respective manufacturer's instructions. Tissue was homogenized with 5 mL of 50 mM PBS buffer (pH 7.2) containing 1 mM EDTA. Homogenates were centrifuged at 500*g* for 5 min at 4 °C and the supernatant was isolated. For measurement of SOD activity, the Cayman's colorimetrical SOD assay utilizes tetazolium salt for detection of superoxide radicals generated by xanthine oxidase and hypoxanthine. The tetazolium salt was transformed to formazan, which can be measured spectrophotometrically at 460 nm with a microplate reader (Tecan) [32]. SOD activity is expressed as the amount of the SOD standard showing activity equivalent to the determined activity. The results are expressed as units (U)/mg protein. For GSH measurement, 200 μL of 0.5 w/v metaphosphoric acid (MPA) was added to all samples for protein precipitation together with 1 mM EDTA to prevent GSH oxidation from transition metals at the desired assay point according to the recommendation of manufacturer [33]. The GSH reacts with 5,5′-dithio-*bis*−2-(nitrobenzoic acid) to produce a yellow colored 5-thio-2-nitrobenzoic acid, which was determined by measuring the absorbance at 405 nm with a microplate reader (Tecan). GSH activity is expressed as the amount of the GSH standard showing activity equivalent to the determined activity.

2.10. Statistical analysis

Data were analyzed with GraphPad Prism-5 statistic software (La Jolla, CA). All values are presented as the mean ± SEM and analyzed by Student's *t*-test (two groups) or ANOVA followed by Tukey post-hoc test (three groups or more). $P < 0.05$ was considered statistically significant.

3. Results

3.1. Dysfunction of CAP aggravates neointimal hyperplasia after vascular injury

The α7nAChR-KO mouse was used as an animal model with dysfunction of CAP. These mice displayed no differences with respect to body weight, blood glucose, and total cholesterol compared with WT mice under normal chow diet (Fig. 1A-C). The systolic blood pressure of α7nAChR-KO mice was also similar to WT mice (Fig. 1D). To address the role of CAP in vascular injury, the left carotid arteries of α7nAChR-KO and age-matched WT mice were injured to induce neointimal hyperplasia (Fig. 1E). After the injury, the media areas in WT and α7nAChR-KO mice slightly increased, while there was no difference of medial area between WT and α7nAChR-KO mice ($P < 0.05$, Fig. 1F). However, the neointimal areas in α7nAChR-KO mice were remarkably larger than those in WT mice ($P < 0.01$, Fig. 1G). These data indicated that systemic dysfunction of CAP aggravates neointimal hyperplasia after vascular injury in mice.

3.2. Dysfunction of CAP promotes vascular remodeling after vascular injury

Next, we compared the vascular remodeling between WT and α7nAChR-KO mice. As shown in Fig. 2A, Masson staining showed that the number of collagen fibers (stained blue) was much more in the arteries of α7nAChR-KO mice compared with WT mice (~2.7-folds, $P < 0.01$). Immunohistochemistry staining of α-SMA, a marker of VSMCs, demonstrated a remarkable increase of VSMCs number in the neointimal layer α7nAChR-KO mice ($P < 0.01$, Fig. 2B). Moreover, immunohistochemistry staining of PCNA (a marker of proliferation) showed the proliferative cells in injured arteries of α7nAChR-KO mice were much more than WT mice ($P < 0.01$, Fig. 2C). We performed immunoblotting of α-SMA and PCNA in the extract of injured arteries, and confirmed that both of α-SMA and PCNA protein levels were significantly higher in α7nAChR-KO mice compared with WT mice ($P < 0.05$, Fig. 2D). These results suggest that dysfunction of CAP further promotes VSMCs phenotype switch and vascular remodeling.

3.3. Dysfunction of CAP drives arterial inflammation in the neointima

Since CAP plays a crucial role in inflammation regulatory process, we determined the inflammatory factors in the uninjured and injured

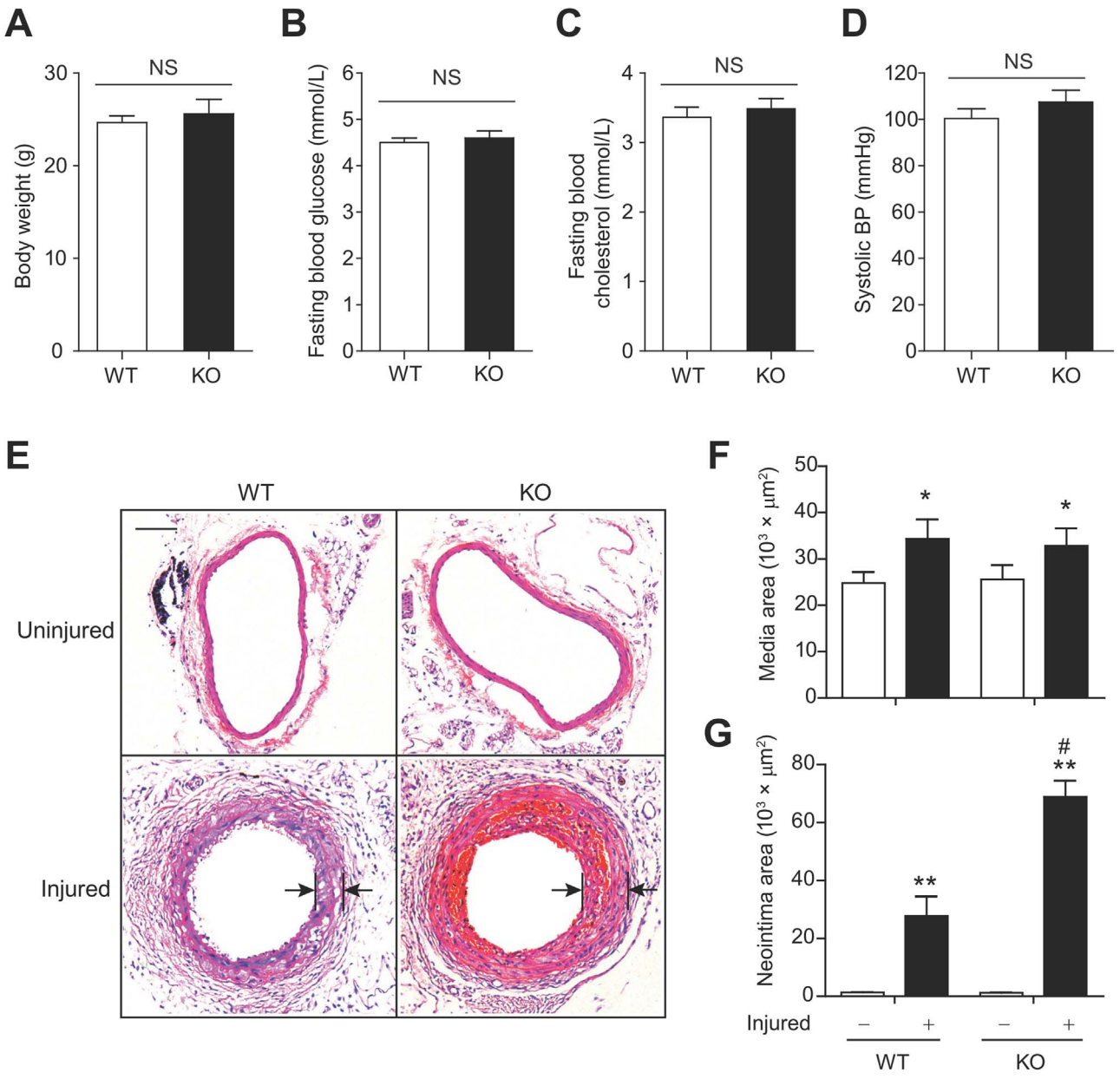

Fig. 1. The neointimal hyperplasia after vascular injury is aggravated in α7nAChR-KO mice. (A-D) Body weight, blood glucose, total cholesterol and systolic blood pressure (BP) in WT and α7nAChR-KO mice. (E) At 4 weeks after vascular injury, the injured left common carotid aortae in WT and α7nAChR-KO mice were illustrated. The uninjured right common carotid aortae served as a control. Representative pictures of hematoxylin and eosin (H & E) staining are shown. Scale bar, 100 μm. (F-G) Morphometric analyses of cross-sectional media area (F) and neointima area (G) were performed in uninjured and injured carotid arteries showing the remarkable increase of neointima in α7nAChR-KO mice relative to WT mice. $^{*}P < 0.05$, $^{**}P < 0.01$ injured vs uninjured. $^{\#}P < 0.05$ KO vs WT. N = 8 per group.

vascular wall. Real-time PCR analysis showed that there were no significant differences of TNF-α and IL-1β mRNA levels between uninjured WT and α7nAChR-KO mice (Fig. 3A). However, the TNF-α and IL-1β mRNA levels in injured arteries of α7nAChR-KO mice were ~3.2-folds and ~5-folds higher than those in WT mice respectively ($P < 0.05$, Fig. 3B). Immunohistochemistry staining of TNF-α and IL-1β confirmed these results: the TNF-α positive ($P < 0.01$, Fig. 3C) and IL-1β positive ($P < 0.05$, Fig. 3D) areas in arteries of α7nAChR-KO mice were increased significantly compared with WT mice. We also determined the expression of CD68, a molecular marker for macrophage. The CD68 mRNA level in aortic tissue of KO mice was significantly higher than that in aortic tissue of WT mice (Fig. 3E). Accordingly, the α7nAChR-KO mice displayed more $CD68^{+}$ area in media and intima compared with WT mice ($P < 0.01$, Fig. 3F). In contrast, the $CD68^{+}$ area in adventitia of α7nAChR-KO mice was less than WT mice (Fig. 3F). These suggest that the macrophage infiltration-associated arterial inflammation in aortic tissue is accelerated in α7nAChR-KO mice.

3.4. Dysfunction of CAP arguments the chemokines induction in the neointima

We further examined the expression of CCL2 and CXCL2, two chemokines known to recruit inflammatory macrophages into vascular wall [34]. Both Real-time PCR and immunohistochemistry staining showed that the levels of CCL2 mRNA ($P < 0.01$, Fig. 4A) and protein ($P < 0.01$, Fig. 4B) in α7nAChR-KO mice aortae were significantly higher than those in WT mice. Similar expression pattern of CXCL2 mRNA ($P < 0.05$, Fig. 4C) and protein ($P < 0.01$, Fig. 4D) was observed in the injured arteries from WT and α7nAChR-KO mice. These data indicate that dysfunction of CAP arguments the chemokines induction

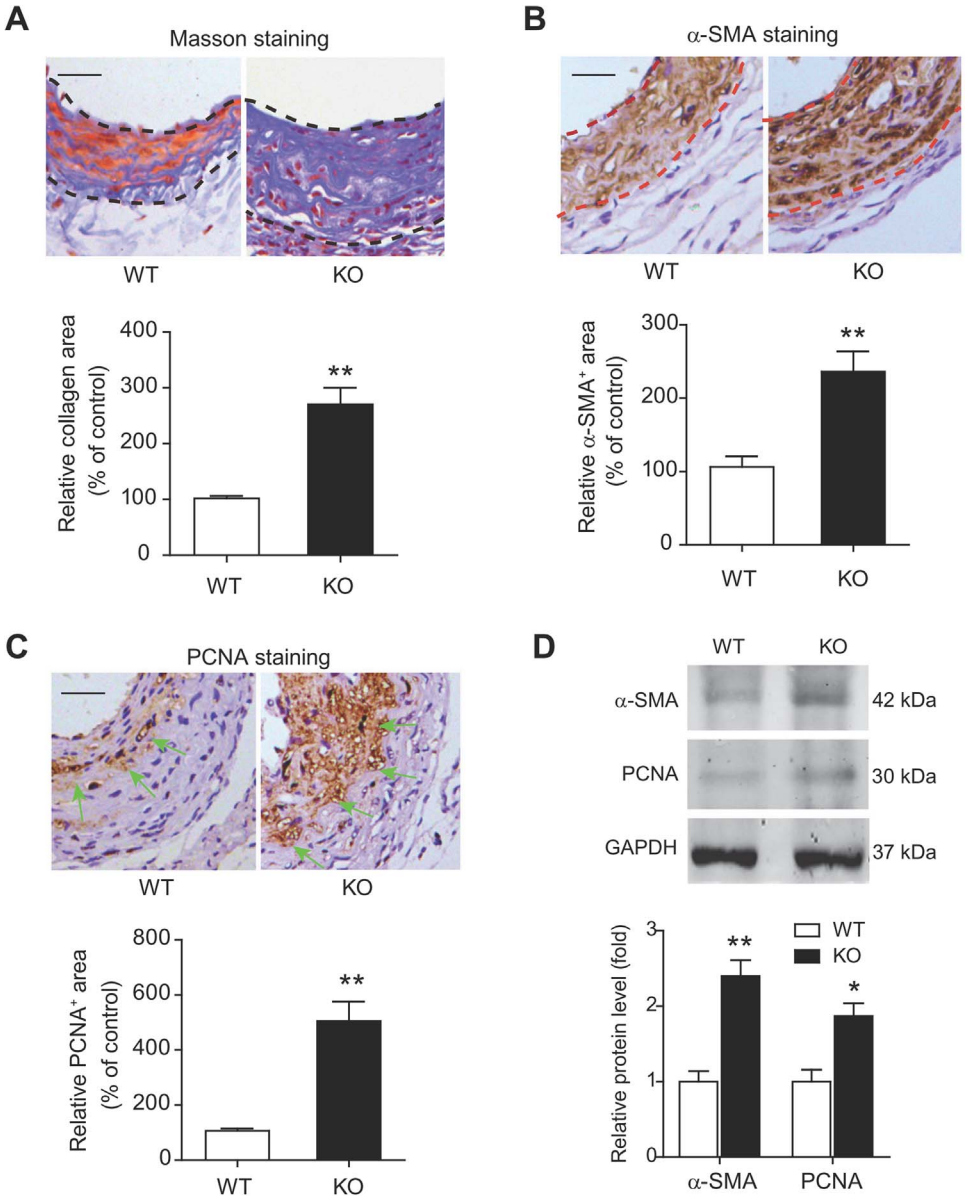

Fig. 2. The vascular remodeling after vascular injury is accelerated in α7nAChR-KO mice. (A) Representative images and quantitative results of Masson staining in injured carotid arteries of WT and α7nAChR − KO mice. The blue areas indicate collagen fibers, while the red areas indicate smooth muscle tissue. The number of collagen fibers is significantly higher in α7nAChR − KO mice compared with WT mice. (B) Representative images and quantitative results of α-SMA immunohistochemical staining in injured carotid arteries of WT and α7nAChR − KO mice. The brown areas indicate positive α-SMA staining. The α-SMA staining positive areas in α7nAChR − KO mice are significantly larger than WT mice. (C) Representative images and quantitative results of PCNA immunohistochemical staining in injured carotid arteries of WT and α7nAChR − KO mice. The brown areas indicate positive PCNA staining. The PCNA staining positive areas in α7nAChR − KO mice are significantly larger than WT mice. (D) Immunoblotting analysis of α-SMA and PCNA in aortic tissues showing significant upregulation of α-SMA and PCNA in α7nAChR − KO mice aortae compared with WT mice. $^{*}P < 0.05$, $^{**}P < 0.01$ KO vs WT. N = 8 per group. Scale bar, 30 μm (For interpretation of the references to color in this figure legend, the reader is referred to the web version of this article.).

in arteries after vascular injury.

3.5. Dysfunction of CAP enhances oxidative stress in the injured aortae

We next determined the oxidative stress. GSH and SOD are two factors both involved in the elimination of free radicals [35]. The results showed that the GSH and SOD levels in injured aortae of α7nAChR-KO mice were lower by ~55% and ~60% compared with WT mice respectively ($P < 0.01$, Fig. 5A). MPO is a peroxidase enzyme released as a response to various stimulatory substances and it most abundantly exists in neutrophil granulocytes and promotes neointima formation in mice [36]. Immunohistochemistry staining of MPO showed that the aortae from α7nAChR-KO mice showed more MPO^{+} area compared with WT mice ($P < 0.01$, Fig. 5B). Immunohistochemistry staining of malondialdehyde (MDA), a product of lipid peroxidation and prostaglandin biosynthesis, demonstrated that the MDA^{+} area was significantly greater in KO mice than WT mice (Fig. 5C). Additionally, we determined 3-nitrotyrosine (3-NT), a marker for the reactive nitrogen oxide species. Both immunoblotting (Fig. 5D) and immunohistochemistry staining (Fig. 5E) showed that the expression of 3-NT in aortic tissue of KO mice was significantly higher than that in WT mice. Finally, we measured protein expression of Nox1, Nox2 and Nox4, three isoforms found in VSMCs generating superoxide anion and hydrogen peroxide [37–39]. Immunoblotting assay demonstrated Nox1, Nox2 and Nox4 were significantly unregulated in injured conditions and to greater extent in α7nAChR-KO mice compared with WT mice ($P < 0.01$, Fig. 5F). These data indicate that dysfunction of CAP enhances oxidative stress in the injured aortae after vascular injury.

3.6. Pharmacologically activation of CAP inhibits neointima formation and arterial inflammation after vascular injury

Next, we tested whether pharmacologically activation of CAP would affect the neointima formation after vascular injury. Four-week administration of PNU-282987, a selective agonist of α7nAChR, successfully reduced the neointima area after vascular injury in mice ($P < 0.01$, Fig. 6A). Immunohistochemistry staining showed that the numbers of $CD68^{+}$ macrophages in injured arteries were also reduced by PNU-282987 administration ($P < 0.01$, Fig. 6B). In line with the decrease number of infiltrated pro-inflammatory cells, the mRNA levels of pro-inflammatory factors TNF-α and IL-1β were also significantly

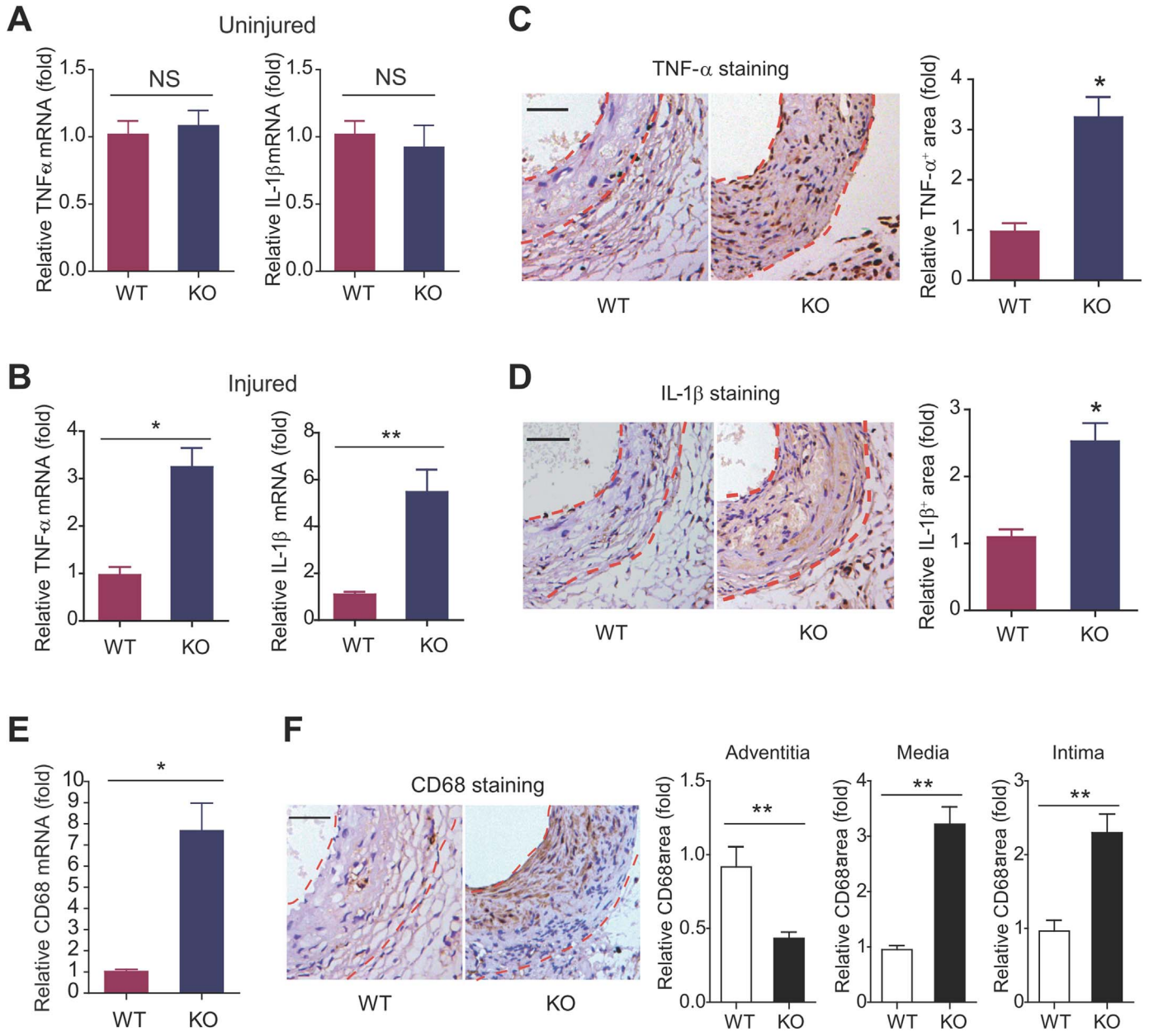

Fig. 3. The arterial inflammation after vascular injury after vascular injury is further enhanced in α7nAChR-KO mice. (A-B) Real-time PCR assay showing the mRNA levels of TNF-α and IL-1β in uninjured (A) or injured (B) carotid arteries of WT and α7nAChR − KO mice. (C-D) Immunohistochemistry assay showing the protein levels of TNF-α (C) and IL-1β (D) in injured carotid arteries of α7nAChR − KO mice were higher than those in WT mice aortae. (E) The mRNA level of macrophage marker CD68 in injured carotid arteries from WT and α7nAChR − KO mice. (F) Representative images of immunohistochemical staining on macrophage marker CD68 in adventitia, media and intima of injured carotid arteries from WT and α7nAChR − KO mice. *$P < 0.05$, **$P < 0.01$ KO vs WT. N = 8 per group. Scale bar, 30 μm.

downregulated in arteries of PNU-282987-treated mice ($P < 0.01$, Fig. 6C). Further, PNU-282987 treatment inhibited the chemokines CCL2 and CXCL2 expression in injured arteries ($P < 0.01$, Fig. 6D). All these results indicate that pharmacologically activation of CAP inhibits neointima formation and arterial inflammation after vascular injury.

3.7. Pharmacologically activation of CAP suppresses oxidative stress in the injured aortae

Finally, we examined the influence of pharmacologically activation of CAP on oxidative stress. The SOD and GSH levels in injured aortae were significantly lower than that in uninjured aortae; however, PNU-282987 treatment partly rescued the SOD and GSH levels ($P < 0.01$, Fig. 7A). In addition, immunoblotting assay showed that the increased protein level of 3-NT in injured aortae were suppressed by PNU-282987 treatment ($P < 0.01$, Fig. 7B). In the uninjured aortae, 3-NT, MDA and MPO staining were scarce ($P < 0.01$, Figs. 7C, 7D and 7E respectively). In the injured aortae, 3-NT, MDA and MPO staining areas (brown) were obviously increased ($P < 0.01$, Figs. 7C, 7D and 7E respectively). PNU-282987 treatment significantly reduced the 3-NT, MDA and MPO expression in the injured aortae ($P < 0.01$, Figs. 7C, 7D and 7E respectively). All these results suggest that activation of CAP suppresses oxidative stress in the injured aortae.

4. Discussion

In this study, we studied the role of CAP in neointima formation, arterial inflammation and oxidative stress after vascular injury. The major findings of our study included: (i) knockout of α7nAChR significantly aggravated neointimal hyperplasia after vascular injury; (ii)

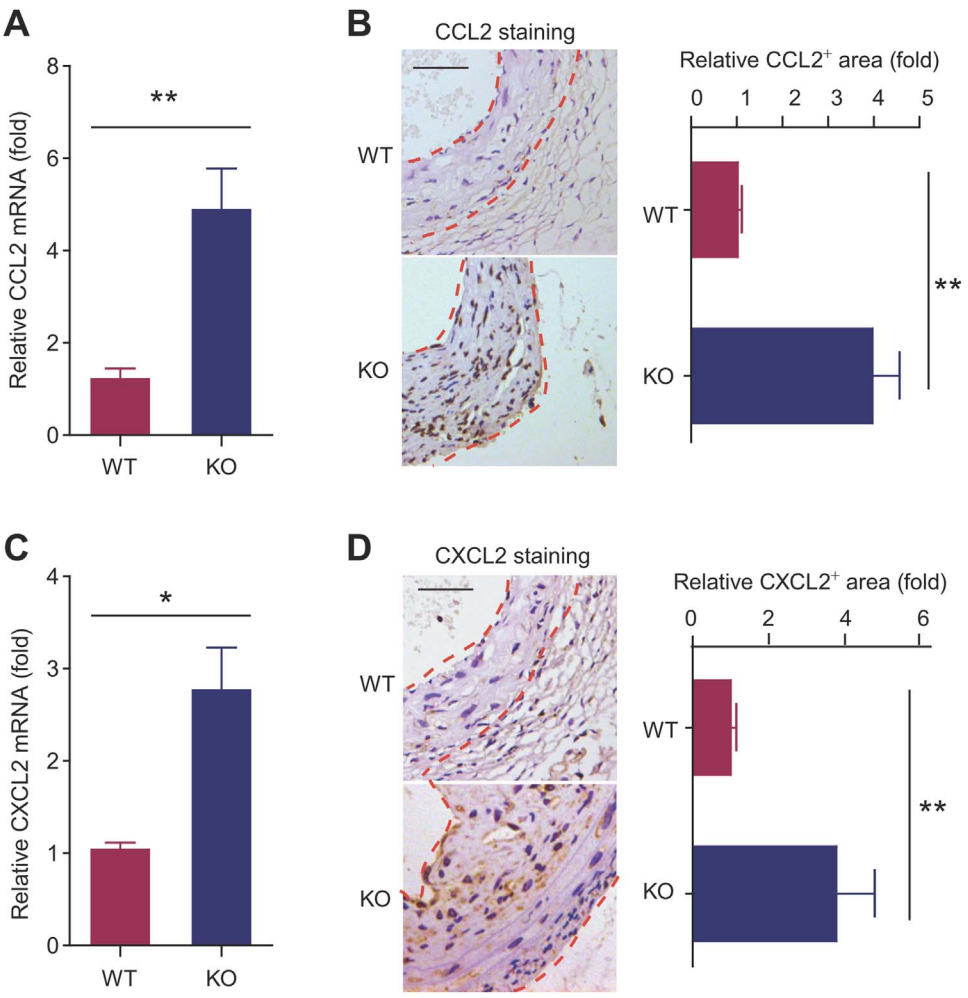

Fig. 4. The chemokines induction after vascular injury is enhanced in α7nAChR-KO mice. (A) Real-time PCR showing the mRNA level of CCL2 in injured carotid arteries of α7nAChR − KO mice was higher than that in WT mice aortae. (B) Immunohistochemistry staining assay showing the protein level of CCL2 in injured carotid arteries of α7nAChR − KO mice was higher than that in WT mice aortae. (C) Real-time PCR showing the mRNA level of CXCL2 in injured carotid arteries of α7nAChR − KO mice was higher than that in WT mice aortae. (D) Immunohistochemistry staining assay showing the protein level of CXCL2 in injured carotid arteries of α7nAChR − KO mice was higher than that in WT mice aortae. $^{*}P < 0.05$, $^{**}P < 0.01$ KO vs WT. N = 8 per group. Scale bar, 30 μm.

knockout of α7nAChR promoted vascular remodeling, arterial inflammation and chemokines induction after vascular injury; (iii) knockout of α7nAChR triggers oxidative stress in the neointima; (iv) pharmacologically activation of CAP with PNU-282987 reduced neointima formation after vascular injury; (v) pharmacological activation of CAP with PNU-282987 inhibited inflammation and oxidative stress. Overall, our results provide evidence that CAP plays a critical role in neointima formation via regulating inflammation and oxidative stress after vascular injury (Fig. 8).

The vagus nerve-based CAP has been discovered in intestinal inflammatory disease for more than 10 years [14–16]. It acts as an endogenous mediator to inhibit the excessive and extensive inflammation in gastrointestinal tract-induced by lipopolysaccharide [14–16]. Importantly, α7nAChR plays a central role in CAP. Activation of α7nAChR by selective agonist not only shows anti-inflammatory effects in intestinal inflammatory disease, but also in other inflammation-related diseases, including sepsis [40], autoimmune myocarditis [41], acute lung injury [42], Fas-induced liver apoptosis [43] and rheumatoid arthritis [44]. In our view, the neointimal hyperplasia after vascular injury may be viewed as an inflammation-related process in response to the mechanical damage, with intimal layer thickening, VSMC proliferation and matrix deposition [2,3]. As an endogenous anti-inflammatory mechanism, it is reasonable to speculate that CAP may participate in the process of neointimal hyperplasia. As expected, the α7nAChR KO mice displayed enhanced neointimal hyperplasia, accelerated arterial inflammation, aggravated pro-inflammatory cells infiltration and further upregulation of chemokines. These phenotypes are totally in agreement with the anti-inflammatory characteristic of CAP in cardiovascular system which was showed by us previously [17–19,21]. Moreover, these results support the viewpoint that CAP inhibits inflammatory reaction in the vascular wall, and thereby may suppress the inflammation-induced local oxidative stress and cellular damage after vascular injury.

Redox and redox-related inflammation play a critical role in vascular dysfunction [45–48]. Due to the anti-inflammatory feature, CAP or α7nAChR also plays critical roles in redox biology. Wilund *et al.* reported that the α7nAChR knockout mice have higher markers of serum oxidative stress such as thiobarbituric acid reactive substances and paraoxonase activities [49]. In the arterial wall of α7nAChR knockout mice, we observed significantly increased oxidative stress markers (MPO, MDA, 3-NT, Nox1, Nox2 and Nox4 levels) and decreased antioxidant enzymes (GSH and SOD levels). Thus, our results are apparently in line with the results from Wilund et al. [49]. α7nAChR is a neuroprotective factor via inhibiting oxidative stress. Activation of α7nAChR exerts neuroprotection by upregulating antioxidant Nrf2/HO-1 pathway [50]. Moreover, activation of α7nAChR limited brain injury by reducing oxidative stress in mice with ischemic stroke [51] and Parkinson's disease [52] respectively. Specifically, compared to the saline-treated mice, mice received α7nAChR activator PHA568487 had fewer behavior deficits at 3 and 7 days after brain ischemia, and smaller lesion volume, fewer $CD68^{+}$ and M1/M2 macrophage ratio at 3 and 14 days after brain ischemia [53]. α7nAChR activator PHA568487 also increased anti-oxidant genes and NADPH oxidase expression associated with decreased phosphorylation of NF-κB p65 isoform in microglia/macrophages [53]. α7nAChR also acts as an anti-inflammatory and anti-oxidant in the periphery. Our previous

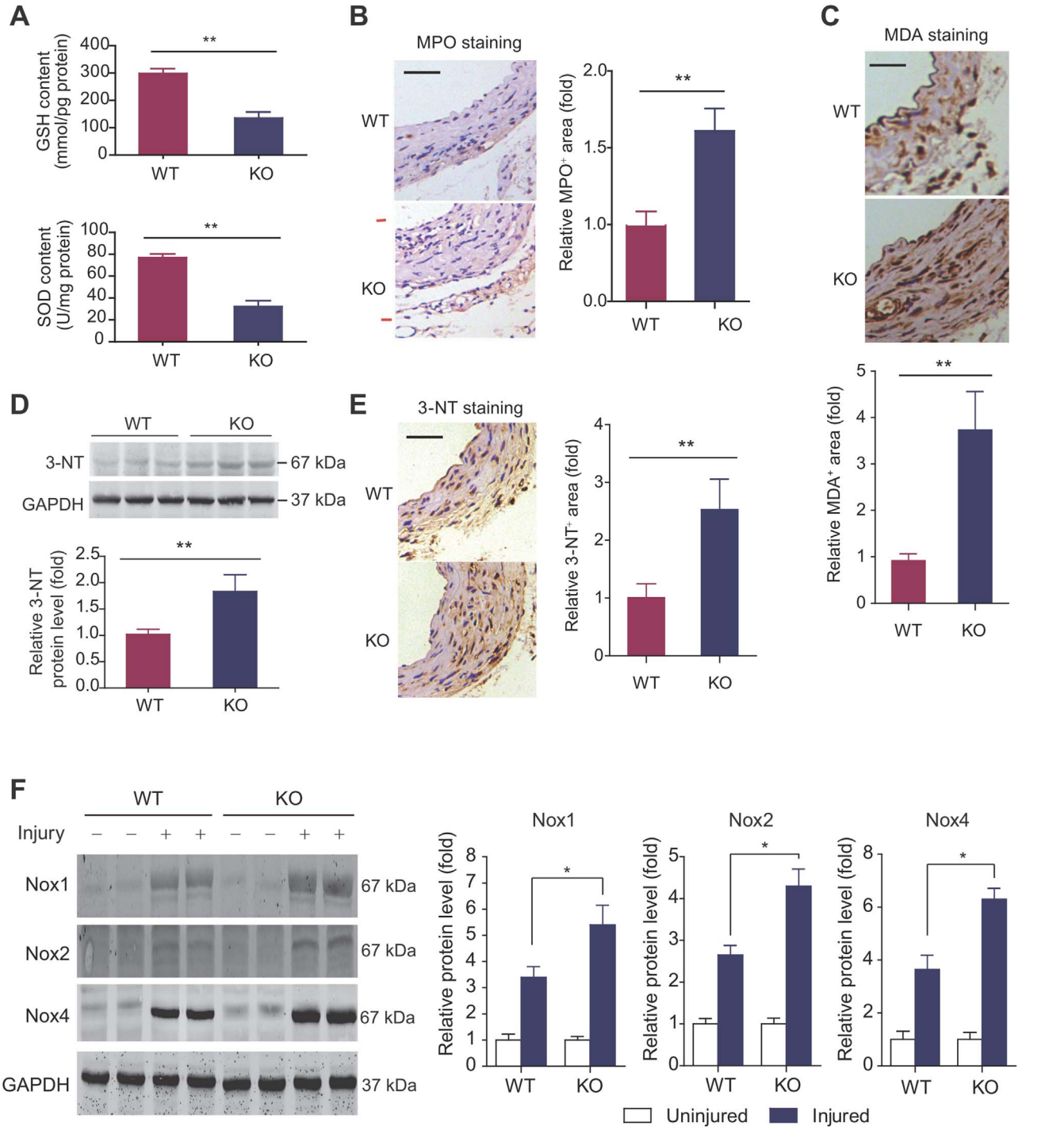

Fig. 5. α7nAChR-KO mice have pronounced oxidative stress in vascular wall after vascular injury compared with WT mice. (A) Comparison of GSH and SOD levels in injured aortic tissues between WT and α7nAChR-KO mice. $^{**}P < 0.01$ KO vs WT. N = 8 per group. (B) Immunohistochemistry staining of MPO in injured aortic tissues from WT and α7nAChR-KO mice. $^{**}P < 0.01$ KO vs WT. N = 8 per group. (C) Immunohistochemistry staining of MDA in injured aortic tissues from WT and α7nAChR-KO mice. $^{**}P < 0.01$ KO vs WT. N = 8 per group. (D-E) Immunoblotting and immunohistochemistry assay of 3-nitrotyrosine (3-NT) in injured aortic tissues from WT and α7nAChR-KO mice. (F) Immunoblotting assay showing the protein expression of Nox1, Nox2 and Nox4 in uninjured and injured aortic tissues from WT and α7nAChR-KO mice. $^{**}P < 0.01$ KO vs WT. N = 8 per group. Scale bar, 30 μm.

study showed activation of α7nAChR not only prevented H_2O_2-mediated cell damage through reducing vascular peroxidase-1 in a JNK signaling-dependent manner in endothelial cells [17], but also suppressed ROS and H_2O_2 on Kupffer cells during hepatic ischemia–reperfusion [54]. In this study, we showed that activation of α7nAChR by PNU-282987 restrained the triggered inflammation and oxidative stress in the injured aortae, further supporting the inhibitory action of α7nAChR on oxidative stress in vascular injury condition such as percutaneous coronary intervention.

Interestingly, nicotine, a non-selective activator of nAChRs and one of the most efficacious compounds in tobacco, seemed to accelerate intimal proliferation and thickening in balloon catheter denuding injured iliac artery and promote the development of restenosis [55]. This effect was reported to be associated with the activation of ERK-Egr-1 signaling cascade by nicotine in VSMCs [56] and enhanced release of basic fibroblast growth factor [57]. Moreover, nicotine instigates formation of abdominal aortic aneurysms in mice [58]. We consider that different nAChRs may mediate distinct actions under nicotine

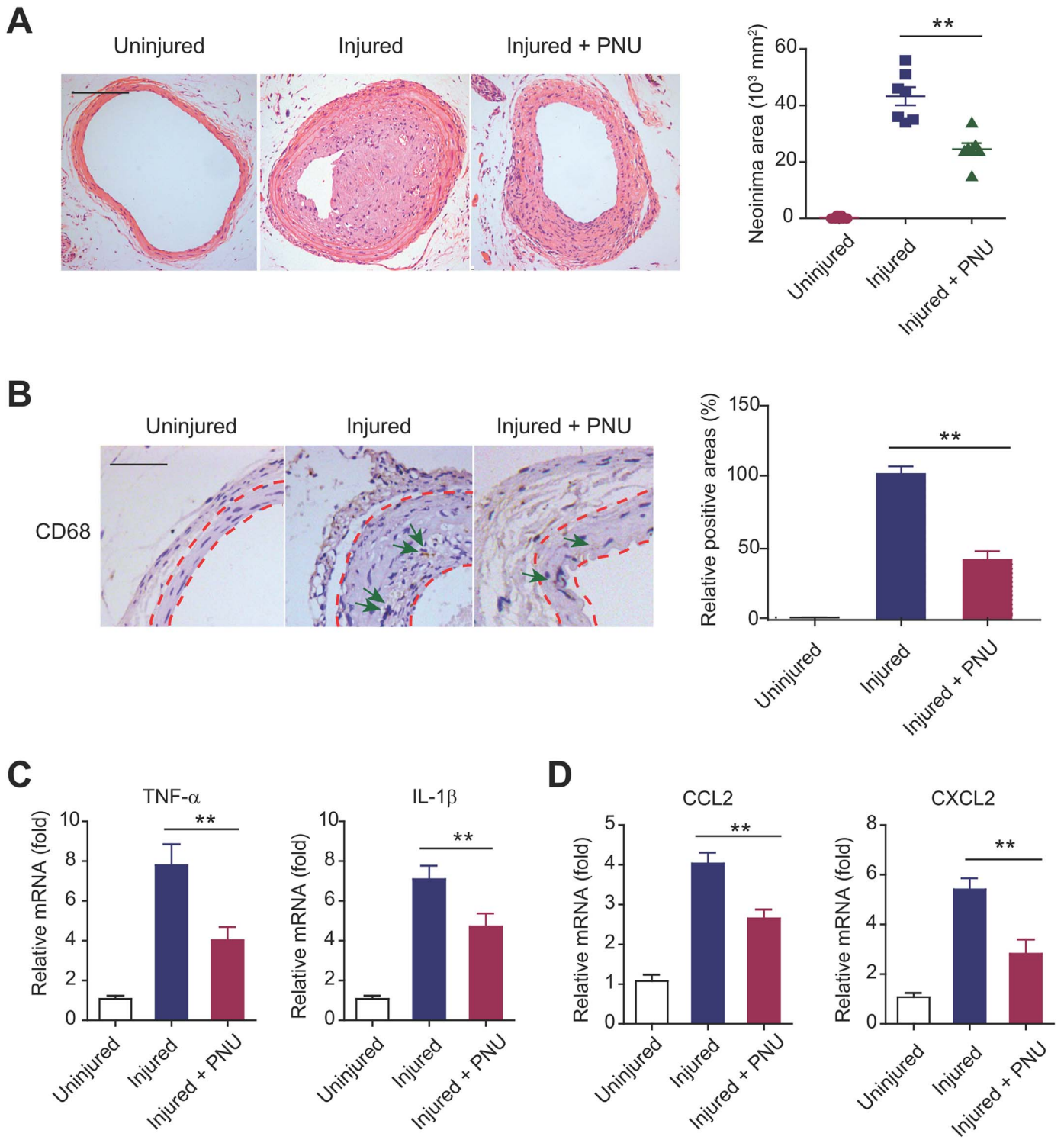

Fig. 6. Activation of CAP inhibits neointimal hyperplasia and inflammation after vascular injury in mice. (A) Effect of activation of CAP with PNU-282987 (1 mg/kg/d, i.p.) administration on neointima formation after vascular injury in C57Bl/6 mice. $^{**}P < 0.01$. N = 8 per group. Scale bar, 100 μm. (B) Immunohistochemistry of CD68 showing the effects of activation of CAP with PNU-282987 administration macrophages infiltration after vascular injury in C57Bl/6 mice. $^{**}P < 0.01$ vs injured. N = 8 per group. Scale bar, 30 μm. (C) The mRNA levels of pro-inflammatory factor TNF-α and IL-1β in aortic tissues after vascular injury in C57Bl/6 mice. $^{**}P < 0.01$ vs injured. N = 8 per group. (D) The mRNA levels of chemokines CCL-2 and CXCL2 in aortic tissues after vascular injury in C57Bl/6 mice. $^{**}P < 0.01$ vs injured. N = 8 per group. PNU, PNU-282987.

activation in vessels. In support of this speculation, Maouche *et al.* showed that only α7nAChR, as opposed to other heteropentameric $\alpha_x\beta_y$nAChRs, controls the proliferation of human airway epithelial basal cells [59]. They found that neither blockade of $\alpha_3\beta_2$nAChR with α-connotoxin, nor blockade of $\alpha_x\beta_y$nAChRs with mecamylamine, affected the proliferation of human airway epithelial basal cells. By contrary, antagonists of α7nAChR stimulated human airway epithelial basal cell proliferation [59]. In addition, Lee *et al.* demonstrated that the atherosclerotic mice with bone marrow deletion of α7nAChR exhibited reduced atherosclerosis plaque size, macrophage infiltration and VSMCs proliferation [60]. As nicotine is not a compound with specific action on α7nAChR, and can activate all types of nAChRs such

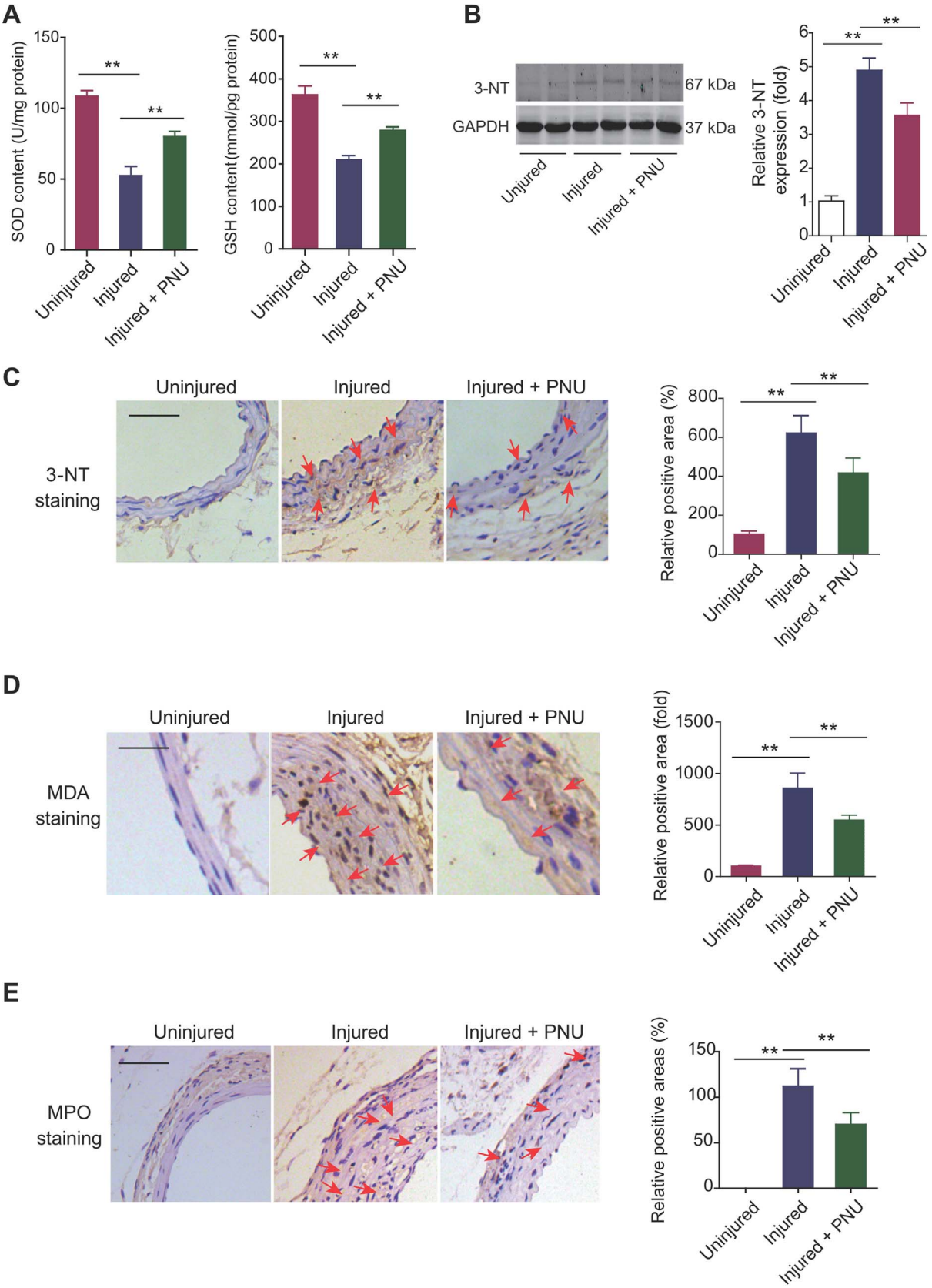

Fig. 7. Activation of CAP inhibits oxidative stress after vascular injury in mice. (A) Effect of activation of CAP with PNU-282987 administration (1 mg/kg/d, i.p.) on SOD and GSH levels in aortic tissues after vascular injury. $^{**}P < 0.01$. N = 8 per group. (B) Immunoblotting assay showing effect of activation of CAP with PNU-282987 administration (1 mg/kg/d, i.p.) on 3-NT protein expression in aortic tissue. $^{**}P < 0.01$. N = 8 per group. (C-E) Immunohistochemistry staining showing the effect of activation of CAP with PNU-282987 administration (1 mg/kg/d, i.p.) on 3-NT, MDA and MPO expression pattern in aortic tissues after vascular injury in mice. $^{**}P < 0.01$. N = 8 per group. PNU, PNU-282987. Scale bar, 30 μm.

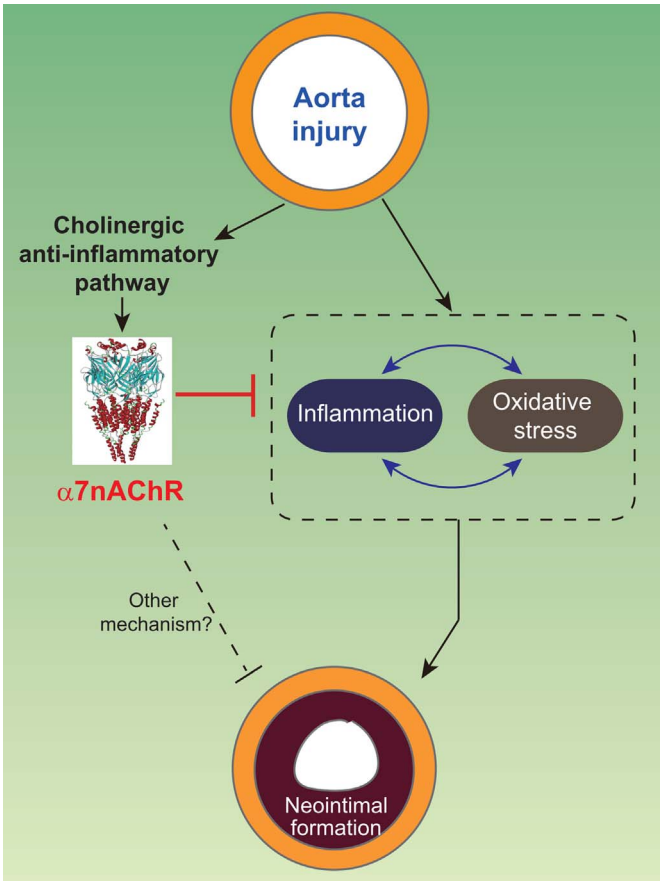

Fig. 8. A working model for activation of cholinergic anti-inflammatory pathway inhibits neointimal hyperplasia via suppressing oxidative stress after vascular injury.

as α3β4nAChR, α3β2nAChR and α34β2nAChR, we think the unfavorable effects of nicotine may be mediated by other nAChRs. To prove this point, further investigations are warranted.

In conclusion, the results in the present study demonstrate that loss of α7nAChR significantly aggravates neointimal hyperplasia after vascular injury, together with enhanced inflammation and oxidative stress. Moreover, pharmacological activation of CAP by α7nAChR agonist reduces neointima formation, arterial inflammation and oxidative stress. These results add new understandings on the pathogenesis of neointimal hyperplasia and indicate α7nAChR may be a promising therapeutic target for management of in-stent stenosis.

Funding

This work was supported by grants from the National Science Foundation of China (No. 81773719, No. 81422049, No. 81473208 and No. 81673485), National 863 Plan Young Scientist Program of China (No. 2015AA020943) and Shanghai Municipal Health and Family Planning Commission Foundation (No. 2016ZB0306).

Conflict of interest

The authors declare no conflicts of interest.

References

[1] V.J. Dzau, R.C. Braun-Dullaeus, D.G. Sedding, Vascular proliferation and atherosclerosis: new perspectives and therapeutic strategies, Nat. Med. 8 (2002) 1249–1256.
[2] C. Chaabane, F. Otsuka, R. Virmani, M.L. Bochaton-Piallat, Biological responses in stented arteries, Cardiovasc. Res. 99 (2013) 353–363.
[3] A.T. Nguyen, D. Gomez, R.D. Bell, J.H. Campbell, A.W. Clowes, et al., Smooth muscle cell plasticity: fact or fiction? Circ. Res. 112 (2013) 17–22.
[4] C.H. Byon, J.M. Heath, Y. Chen, Redox signaling in cardiovascular pathophysiology: a focus on hydrogen peroxide and vascular smooth muscle cells, Redox Biol. 9 (2016) 244–253.
[5] S. Koka, M. Xia, Y. Chen, O.M. Bhat, X. Yuan, et al., Endothelial NLRP3 inflammasome activation and arterial neointima formation associated with acid sphingomyelinase during hypercholesterolemia, Redox Biol. 13 (2017) 336–344.
[6] T. Ashino, M. Yamamoto, T. Yoshida, S. Numazawa, Redox-sensitive transcription factor Nrf2 regulates vascular smooth muscle cell migration and neointimal hyperplasia, Arterioscler. Thromb. Vasc. Biol. 33 (2013) 760–768.
[7] D.H. Kang, D.J. Lee, J. Kim, J.Y. Lee, H.W. Kim, et al., Vascular injury involves the overoxidation of peroxiredoxin type II and is recovered by the peroxiredoxin activity mimetic that induces reendothelialization, Circulation 128 (2013) 834–844.
[8] A.I. Rodriguez, A. Gangopadhyay, E.E. Kelley, P.J. Pagano, B.S. Zuckerbraun, et al., HO-1 and CO decrease platelet-derived growth factor-induced vascular smooth muscle cell migration via inhibition of Nox1, Arterioscler. Thromb. Vasc. Biol. 30 (2010) 98–104.
[9] H. Sies, Hydrogen peroxide as a central redox signaling molecule in physiological oxidative stress: oxidative eustress, Redox Biol. 11 (2017) 613–619.
[10] A.M. Mahmoud, M.M. Ali, E.R. Miranda, J.T. Mey, B.K. Blackburn, et al., Nox2 contributes to hyperinsulinemia-induced redox imbalance and impaired vascular function, Redox Biol. 13 (2017) 288–300.
[11] R. Hurst, H. Rollema, D. Bertrand, Nicotinic acetylcholine receptors: from basic science to therapeutics, Pharmacol. Ther. 137 (2013) 22–54.
[12] M. Bencherif, S.T. Narla, M.S. Stachowiak, Alpha7 neuronal nicotinic receptor: a pluripotent target for diseases of the central nervous system, CNS Neurol. Disord. Drug Targets 13 (2014) 836–845.
[13] K.W. Gee, A. Olincy, R. Kanner, L. Johnson, D. Hogenkamp, et al., First in human trial of a type I positive allosteric modulator of alpha7-nicotinic acetylcholine receptors: pharmacokinetics, safety, and evidence for neurocognitive effect of AVL-3288, J. Psychopharmacol. (2017) (269881117691590).
[14] L.V. Borovikova, S. Ivanova, M. Zhang, H. Yang, G.I. Botchkina, et al., Vagus nerve stimulation attenuates the systemic inflammatory response to endotoxin, Nature 405 (2000) 458–462.
[15] H. Wang, M. Yu, M. Ochani, C.A. Amella, M. Tanovic, et al., Nicotinic acetylcholine receptor alpha7 subunit is an essential regulator of inflammation, Nature 421 (2003) 384–388.
[16] W.J. de Jonge, E.P. van der Zanden, F.O. The, M.F. Bijlsma, D.J. van Westerloo, et al., Stimulation of the vagus nerve attenuates macrophage activation by activating the Jak2-STAT3 signaling pathway, Nat. Immunol. 6 (2005) 844–851.
[17] D.J. Li, T. Zhao, R.J. Xin, Y.Y. Wang, Y.B. Fei, et al., Activation of alpha7 nicotinic acetylcholine receptor protects against oxidant stress damage through reducing vascular peroxidase-1 in a JNK signaling-dependent manner in endothelial cells, Cell Physiol. Biochem. 33 (2014) 468–478.
[18] D.J. Li, R.G. Evans, Z.W. Yang, S.W. Song, P. Wang, et al., Dysfunction of the cholinergic anti-inflammatory pathway mediates organ damage in hypertension, Hypertension 57 (2011) 298–307.
[19] J.K. Chen, T. Zhao, M. Ni, D.J. Li, X. Tao, et al., Downregulation of alpha7 nicotinic acetylcholine receptor in two-kidney one-clip hypertensive rats, BMC Cardiovasc. Disord. 12 (2012) 38.
[20] C. Liu, F.M. Shen, Y.Y. Le, Y. Kong, X. Liu, et al., Antishock effect of anisodamine involves a novel pathway for activating alpha7 nicotinic acetylcholine receptor, Crit. Care Med. 37 (2009) 634–641.
[21] D.J. Li, F. Huang, M. Ni, H. Fu, L.S. Zhang, et al., alpha7 nicotinic acetylcholine receptor relieves angiotensin II-induced senescence in vascular smooth muscle cells by raising nicotinamide adenine dinucleotide-dependent SIRT1 activity, Arterioscler. Thromb. Vasc. Biol. 36 (2016) 1566–1576.
[22] M. Sahara, M. Sata, T. Morita, K. Nakamura, Y. Hirata, et al., Diverse contribution of bone marrow-derived cells to vascular remodeling associated with pulmonary arterial hypertension and arterial neointimal formation, Circulation 115 (2007) 509–517.
[23] H. Lv, Q. Liu, Z. Wen, H. Feng, X. Deng, et al., Xanthohumol ameliorates lipopolysaccharide (LPS)-induced acute lung injury via induction of AMPK/GSK3beta-Nrf2 signal axis, Redox Biol. 12 (2017) 311–324.
[24] S. Yang, L. Zhao, Y. Han, Y. Liu, C. Chen, et al., Probucol ameliorates renal injury in diabetic nephropathy by inhibiting the expression of the redox enzyme p66Shc, Redox Biol. 13 (2017) 482–497.
[25] D.J. Li, Y.H. Li, H.B. Yuan, L.F. Qu, P. Wang, The novel exercise-induced hormone irisin protects against neuronal injury via activation of the Akt and ERK1/2 signaling pathways and contributes to the neuroprotection of physical exercise in cerebral ischemia, Metabolism 68 (2017) 31–42.
[26] A.I. Rojo, M. Pajares, P. Rada, A. Nunez, A.J. Nevado-Holgado, et al., NRF2 deficiency replicates transcriptomic changes in Alzheimer's patients and worsens APP and TAU pathology, Redox Biol. 13 (2017) 444–451.
[27] F. Rezende, C. Schurmann, S. Schutz, S. Harenkamp, E. Herrmann, et al., Knock out of the NADPH oxidase Nox4 has no impact on life span in mice, Redox Biol. 11 (2017) 312–314.
[28] S. Park, J.A. Park, H. Yoo, H.B. Park, Y. Lee, Proteasome inhibitor-induced cleavage of HSP90 is mediated by ROS generation and caspase 10-activation in human leukemic cells, Redox Biol. 13 (2017) 470–476.
[29] P. Wang, R.Y. Zhang, J. Song, Y.F. Guan, T.Y. Xu, et al., Loss of AMP-activated protein kinase-alpha2 impairs the insulin-sensitizing effect of calorie restriction in skeletal muscle, Diabetes 61 (2012) 1051–1061.
[30] P. Wang, H. Du, C.C. Zhou, J. Song, X. Liu, et al., Intracellular NAMPT-NAD +-SIRT1 cascade improves post-ischaemic vascular repair by modulating Notch signalling in endothelial progenitors, Cardiovasc. Res. 104 (2014) 477–488.

[31] N. Li, M. Karaca, P. Maechler, Upregulation of UCP2 in beta-cells confers partial protection against both oxidative stress and glucotoxicity, Redox Biol. 13 (2017) 541–549.
[32] D.S. Salmanoglu, T. Gurpinar, K. Vural, N. Ekerbicer, E. Dariverenli, et al., Melatonin and L-carnitin improves endothelial disfunction and oxidative stress in Type 2 diabetic rats, Redox Biol. 8 (2016) 199–204.
[33] T.A. Theodossiou, C.E. Olsen, M. Jonsson, A. Kubin, J.S. Hothersall, et al., The diverse roles of glutathione-associated cell resistance against hypericin photodynamic therapy, Redox Biol. 12 (2017) 191–197.
[34] I.F. Charo, M.B. Taubman, Chemokines in the pathogenesis of vascular disease, Circ. Res. 95 (2004) 858–866.
[35] F. Ursini, M. Maiorino, H.J. Forman, Redox homeostasis: the Golden Mean of healthy living, Redox Biol. 8 (2016) 205–215.
[36] V. Tiyerili, B. Camara, M.U. Becher, J.W. Schrickel, D. Lutjohann, et al., Neutrophil-derived myeloperoxidase promotes atherogenesis and neointima formation in mice, Int. J. Cardiol. 204 (2016) 29–36.
[37] L.L. Hilenski, R.E. Clempus, M.T. Quinn, J.D. Lambeth, K.K. Griendling, Distinct subcellular localizations of Nox1 and Nox4 in vascular smooth muscle cells, Arterioscler. Thromb. Vasc. Biol. 24 (2004) 677–683.
[38] N. Anilkumar, R. Weber, M. Zhang, A. Brewer, A.M. Shah, Nox4 and nox2 NADPH oxidases mediate distinct cellular redox signaling responses to agonist stimulation, Arterioscler. Thromb. Vasc. Biol. 28 (2008) 1347–1354.
[39] F. Antunes, P.M. Brito, Quantitative biology of hydrogen peroxide signaling, Redox Biol. 13 (2017) 1–7.
[40] V.A. Pavlov, M. Ochani, L.H. Yang, M. Gallowitsch-Puerta, K. Ochani, et al., Selective alpha7-nicotinic acetylcholine receptor agonist GTS-21 improves survival in murine endotoxemia and severe sepsis, Crit. Care Med. 35 (2007) 1139–1144.
[41] C. Leib, S. Goser, D. Luthje, R. Ottl, T. Tretter, et al., Role of the cholinergic anti-inflammatory pathway in murine autoimmune myocarditis, Circ. Res. 109 (2011) 130–140.
[42] X. Su, J.W. Lee, Z.A. Matthay, G. Mednick, T. Uchida, et al., Activation of the alpha7 nAChR reduces acid-induced acute lung injury in mice and rats, Am. J. Respir. Cell Mol. Biol. 37 (2007) 186–192.
[43] T. Hiramoto, Y. Chida, J. Sonoda, K. Yoshihara, N. Sudo, et al., The hepatic vagus nerve attenuates Fas-induced apoptosis in the mouse liver via alpha7 nicotinic acetylcholine receptor, Gastroenterology 134 (2008) 2122–2131.
[44] M.A. van Maanen, S.P. Stoof, G.J. Larosa, M.J. Vervoordeldonk, P.P. Tak, Role of the cholinergic nervous system in rheumatoid arthritis: aggravation of arthritis in nicotinic acetylcholine receptor alpha7 subunit gene knockout mice, Ann. Rheum. Dis. 69 (2010) 1717–1723.
[45] Z. Liu, Y. Liu, Q. Xu, H. Peng, Y. Tang, et al., Critical role of vascular peroxidase 1 in regulating endothelial nitric oxide synthase, Redox Biol. 12 (2017) 226–232.
[46] C. Damacena-Angelis, G.H. Oliveira-Paula, L.C. Pinheiro, E.J. Crevelin, R.L. Portella, et al., Nitrate decreases xanthine oxidoreductase-mediated nitrite reductase activity and attenuates vascular and blood pressure responses to nitrite, Redox Biol. 12 (2017) 291–299.
[47] R. Matsui, Y. Watanabe, C.E. Murdoch, Redox regulation of ischemic limb neovascularization - What we have learned from animal studies, Redox Biol. 12 (2017) 1011–1019.
[48] F. Luchetti, R. Crinelli, E. Cesarini, B. Canonico, L. Guidi, et al., Endothelial cells, endoplasmic reticulum stress and oxysterols, Redox Biol. 13 (2017) 581–587.
[49] K.R. Wilund, M. Rosenblat, H.R. Chung, N. Volkova, M. Kaplan, et al., Macrophages from alpha 7 nicotinic acetylcholine receptor knockout mice demonstrate increased cholesterol accumulation and decreased cellular paraoxonase expression: a possible link between the nervous system and atherosclerosis development, Biochem. Biophys. Res. Commun. 390 (2009) 148–154.
[50] E. Parada, J. Egea, I. Buendia, P. Negredo, A.C. Cunha, et al., The microglial alpha7-acetylcholine nicotinic receptor is a key element in promoting neuroprotection by inducing heme oxygenase-1 via nuclear factor erythroid-2-related factor 2, Antioxid. Redox Signal. 19 (2013) 1135–1148.
[51] Z. Han, L. Li, L. Wang, V. Degos, M. Maze, et al., Alpha-7 nicotinic acetylcholine receptor agonist treatment reduces neuroinflammation, oxidative stress, and brain injury in mice with ischemic stroke and bone fracture, J. Neurochem. 131 (2014) 498–508.
[52] Y. Liu, X. Zeng, Y. Hui, C. Zhu, J. Wu, et al., Activation of alpha7 nicotinic acetylcholine receptors protects astrocytes against oxidative stress-induced apoptosis: implications for Parkinson's disease, Neuropharmacology 91 (2015) 87–96.
[53] Z. Han, F. Shen, Y. He, V. Degos, M. Camus, et al., Activation of alpha-7 nicotinic acetylcholine receptor reduces ischemic stroke injury through reduction of pro-inflammatory macrophages and oxidative stress, PLoS One 9 (2014) e105711.
[54] M. Ni, H. Fu, F. Huang, T. Zhao, J.K. Chen, et al., Vagus nerve attenuates hepatocyte apoptosis upon ischemia-reperfusion via alpha7 nicotinic acetylcholine receptor on kupffer cells in mice, Anesthesiology 125 (2016) 1005–1016.
[55] Y. Ruixing, B. Qi, L. Tangwei, L. Jiaquan, Effects of nicotine on angiogenesis and restenosis in a rabbit model, Cardiology 107 (2007) 122–131.
[56] R.I. Vazquez-Padron, D. Mateu, L. Rodriguez-Menocal, Y. Wei, K.A. Webster, et al., Novel role of Egr-1 in nicotine-related neointimal formation, Cardiovasc. Res. 88 (2010) 296–303.
[57] A. Cucina, A. Fuso, P. Coluccia, A. Cavallaro, Nicotine inhibits apoptosis and stimulates proliferation in aortic smooth muscle cells through a functional nicotinic acetylcholine receptor, J. Surg. Res. 150 (2008) 227–235.
[58] S. Wang, C. Zhang, M. Zhang, B. Liang, H. Zhu, et al., Activation of amp-activated protein kinase alpha2 by nicotine instigates formation of abdominal aortic aneurysms in mice in vivo, Nat. Med. 18 (2012) 902–910.
[59] K. Maouche, M. Polette, T. Jolly, K. Medjber, I. Cloez-Tayarani, et al., {alpha}7 nicotinic acetylcholine receptor regulates airway epithelium differentiation by controlling basal cell proliferation, Am. J. Pathol. 175 (2009) 1868–1882.
[60] R.H. Lee, G. Vazquez, Reduced size and macrophage content of advanced atherosclerotic lesions in mice with bone marrow specific deficiency of alpha 7 nicotinic acetylcholine receptor, PLoS One 10 (2015) e0124584.